

Nonstationary Phenomena in Tapered Gyro-Backward-Wave Oscillators

G. S. Nusinovich

Institute for Research in Electronics and Applied Physics, University of Maryland, College Park, Maryland 20742

A. N. Vlasov

Science Applications International Corporation, McLean, Virginia 22102

T. M. Antonsen, Jr.

Institute for Research in Electronics and Applied Physics, University of Maryland, College Park, Maryland 20742

(Received 11 January 2001; published 31 October 2001)

Recently, it was found that a gyro-backward-wave oscillator (gyro-BWO) with a tapered waveguide can exhibit stationary oscillations at currents which exceed the starting current by more than 2 orders of magnitude. This result, at first glance, contradicts the theory of transients in untapered linear-beam BWO's, which predicts nonstationary oscillations at currents exceeding the start current by a factor of 3. To explain this behavior of the tapered gyro-BWO, its nonstationary theory is developed. The results obtained demonstrate the consistency of the tapered gyro-BWO operation with the known theory of transients and also show that the tapering may provide stationary oscillations at high currents.

DOI: 10.1103/PhysRevLett.87.218301

PACS numbers: 84.40.Ik, 52.59.Rz, 84.40.Fe

The gyro-backward-wave oscillator (gyro-BWO) is a tunable source of coherent radiation in which electrons gyrating in an external magnetic field interact with an oppositely propagating electromagnetic (EM) wave. Frequency tunability in the gyro-BWO can be realized by varying either the magnetic field, or the beam voltage, or both simultaneously. Such frequency-tunable sources of high-power, millimeter-wave radiation can be of interest for position selective heating, current drive, and stabilization of instabilities in controlled fusion plasma experiments as well as for other applications. The history of the development of gyro-BWO's was recently reviewed in papers [1,2].

In the gyro-BWO, as well as in the conventional BWO driven by a linear electron beam, electrons and EM waves propagating in opposite directions form a feedback loop. Therefore, both the gyro-BWO and the BWO belong to a wide class of active systems with internal distributed feedback. Note that the gyromonotron as well as its linear-beam counterpart, the orotron [3,4], also belong to this class because the EM field excited near cutoff in these devices consists of waves slowly propagating in both directions. So the waves propagating backward can form along with the electrons a feedback loop, similar to that in the gyro-BWO.

Our present work was motivated by recent theoretical [2] and experimental [5] studies of the gyro-BWO. In these studies it was shown, both theoretically and experimentally, that in the gyro-BWO, whose interaction circuit consists of a regular waveguide with uptapers at both ends, the oscillations can be stable even when the beam current exceeds the starting value by about 250 times. (Note that in Ref. [2] only the stationary theory was developed, so the stability issue was not addressed.)

In contrast to this result, previous studies of conventional backward-wave oscillators, BWO's [6–8], clearly

indicated that in the BWO with a uniform slow-wave structure, oscillations with constant amplitude become unstable when the beam current exceeds the starting current by about 3 times. With a further increase in current, as was shown experimentally [8], the device exhibits a sequence of transitions to stochastic oscillations, which agrees well with the known Ruelle-Takens concept [9]. Coming back to gyro-BWO's, we should emphasize that the physical processes in gyro-BWO's are quite similar to those in conventional BWO's. Even more, as shown in Ref. [10], in some cases the equations for the gyro-BWO can be reduced to those for the conventional BWO, in spite of the difference in interaction mechanisms responsible for the coherent EM radiation in both devices. Therefore, it would be reasonable to expect that the performance of the gyro-BWO with a nontapered waveguide should be quite similar to that of a conventional BWO with a uniform slow-wave structure. In contrast to this, the results given in Refs. [2] and [5] demonstrated stable oscillations at very high ratios of the beam current to its starting value. Since in Refs. [2] and [5] the tapered gyro-BWO was studied, this difference, of course, can be attributed to the effect of tapering. In any case, the lack of the stability analysis and of the analysis of transition from tapered to untapered waveguides in Refs. [2] and [5] made a direct comparison of these studies with known studies of conventional BWO's impossible.

To determine the reason for this contradiction, we carried out an analysis of nonstationary processes in the gyro-BWO with various degrees of tapering. To the best of our knowledge, this is the first relatively systematic study of nonstationary processes in such devices, although some results of nonstationary calculations were presented in Ref. [11].

In our simulations we used the code MAGY [12], which has been demonstrated to be an efficient tool for analyzing the physical processes in fast- and slow-wave sources of coherent EM radiation. In our studies we used the parameters of the gyro-BWO studied in Refs. [2] and [5]. The schematic of the gyro-BWO under study is shown in Fig. 1 reproduced from Ref. [2]. In our study we varied the radius of the input uptaper, R_t , the beam current, I_b , and, in some cases, the external magnetic field, B .

Nonstationary processes, which may occur in the device with a given R_t (2.76 mm) and $B = 14.52$ kG, for different currents are illustrated by Fig. 2. Here we plot the electromagnetic wave power at $z = 0$ versus time for nine different values of current. (Power is negative due to the backward-wave propagation.) For currents below the start current, $I_{st} \cong 0.03$ A, the power asymptotically decays to zero (no stable oscillations are observed). Stationary oscillations, as illustrated in Figs. 2a ($I_b = 0.05$ A) and 2b ($I_b = 0.2$ A), are observed in the range $0.03 \leq I_b \leq 0.5$ A. For higher currents the stationary oscillations are replaced by one period automodulation as illustrated by Fig. 2c for $I_b = 0.6$ A. As Fig. 2 plots the power envelope, the output electric field is two frequency quasiperiodic consisting of a carrier signal at 35 GHz modulated at 0.25 GHz. At still higher currents, as illustrated by Figs. 2d (1 A) and 2e (1.5 A), the modulation acquires additional frequencies. As current is raised further, the device returns to regular automodulation, which is shown in Fig. 2f for $I_b = 1.9$ A. Then, in the range of currents from 1.97 A to about 10 A the system exhibits stationary oscillations, examples of which are shown in Figs. 2g for $I_b = 2$ A and 2h for $I_b = 10$ A. At even higher currents the oscillations again become nonstationary, as shown in Fig. 2i for $I_b = 20$ A.

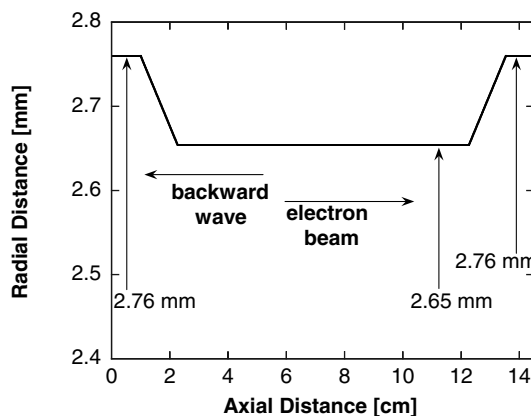


FIG. 1. Configuration of the TE_{11} mode gyro-BWO under study. The input downtaper consists of a 1 cm long section of 2.76 mm radius, followed by a 1.27 cm long downtapered section. The latter, in turn, is followed by a 10 cm long regular waveguide of 2.65 mm radius, which is ended by a symmetric uptaper. The device is nominally driven by a 100 kV, 5 A electron beam with the orbital-to-axial velocity ratio of 1.

The results of simulations done for the magnetic field of 14.52 kG and different values of uptaper are summarized in Fig. 3. This figure shows the plane of parameters “beam current, I_b , versus the radius of the input uptaper, R_t ,” in which the regions of stable stationary oscillations with constant amplitude are shown. The lower line in this map shows the start current of the device. The case $R_t = 2.65$ mm corresponds to an untapered interaction region and we note for this case stationary oscillations are obtained only in the range 0.02 A = $I_{st} \leq I_b \leq 0.08$ A = $4I_{st}$. For tapered circuits the region of parameter space, where stationary oscillations of the type depicted in Fig. 2g exist, is found roughly between 2.69 and 2.77 mm. Approximately 300 different parameter pairs were considered in the construction of Fig. 3. Thus, the precise location of the boundaries is not known.

The axial structure of the EM field excited in the two regions of stationary oscillations is quite different. This statement is illustrated by Fig. 4 showing these axial structures in the device with $R_t = 2.72$ mm for $I_b = 0.1$ A (Fig. 4a) and for $I_b = 1.5$ A (Fig. 4b). At 0.1 A the axial structure is typical for backward-wave oscillations: the field amplitude is largest where the beam enters the interaction region, and this field represents a backward wave since

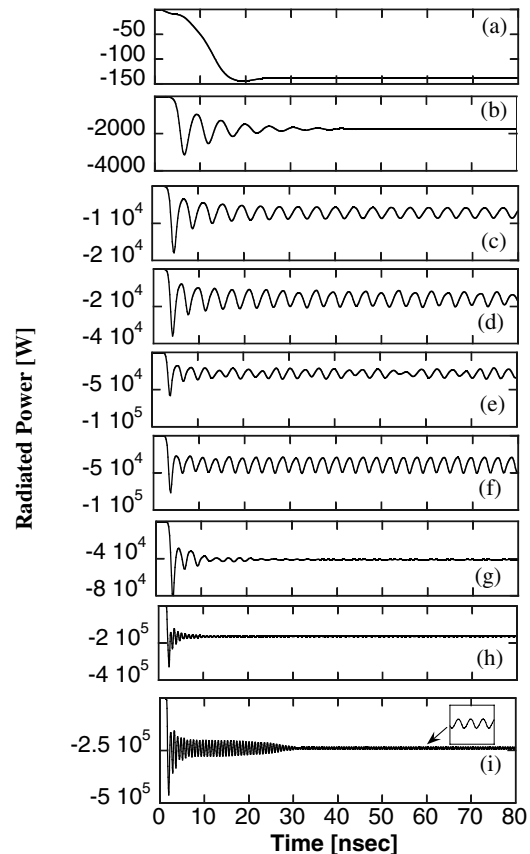


FIG. 2. Nonstationary processes in the gyro-BWO with $R_t = 2.76$ mm at different currents (minus for radiated power indicates the backward propagation of the radiation). See text.

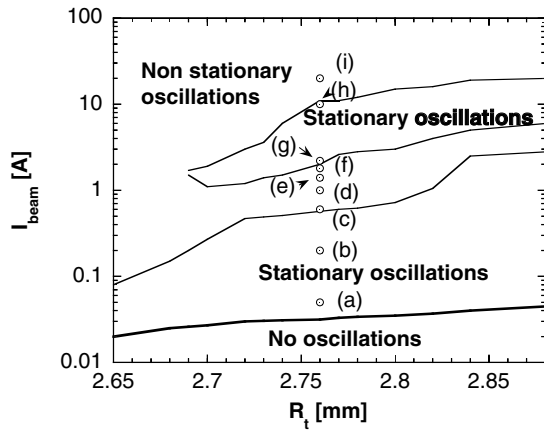


FIG. 3. The gyro-BWO map showing the regions of stationary oscillations with constant amplitude in the parameters’ plane “beam current, I_b , versus uptaper radius, R_t .”

the phase decreases in the z direction. At $I_b = 1.5$ A the field exhibits the self-contraction found in Ref. [2]. The most important peak is localized at $z < 6$ cm, whereas in Fig. 4a the field is large for $z \leq 11$ cm. The second axial variation localized between 6 and 10 cm differs in phase by about π from the first one, and the rest of the waveguide is occupied by a forward wave having a small amplitude. Typically, in the second zone of stationary oscillations the region of self-contraction of the EM field varies from 5 to 6 cm. It seems reasonable to expect that such a mode located at about 5 cm distance should have a much higher starting current than the mode occupying all the waveguide which is about 15 cm long. If, for crude estimates, we assume that the starting current of the gyro-BWO scales with the interaction length L as $I_{st} \sim 1/L^3$, as in conventional BWO’s [13], then the shortening of the length from 15 to 5 cm should increase the starting current from about 0.02 A found in [2] to about 0.5 A. Then, the stable operation at 1.5 A shown in Fig. 4b corresponds to the beam current—to start the current ratio of about 3, which is consistent with the known theory of transients [6]. Coming back to Fig. 3 let us note that at taper radii, where the second stationary region exists, the first mode loses its stability just at beam currents of about 0.5–0.6 A. So the automodulation between the two stationary regions can be attributed to the competition between two modes with different axial structures.

Certainly, the existence of the second stationary zone only at large enough R_t ’s indicates that the uptaper plays an important role in the formation of the self-contracted mode. One of the factors, which can be important for this formation, is the reflection from a backward to a forward wave that occurs at the transition region. This reflection is important because the waveguide is close to cutoff and the electron beam interacts with both the forward and the backward propagating waves. We have conducted simulations for constant radius waveguides, but with specified reflection coefficients at the entrance ($z = 0$). These simulations

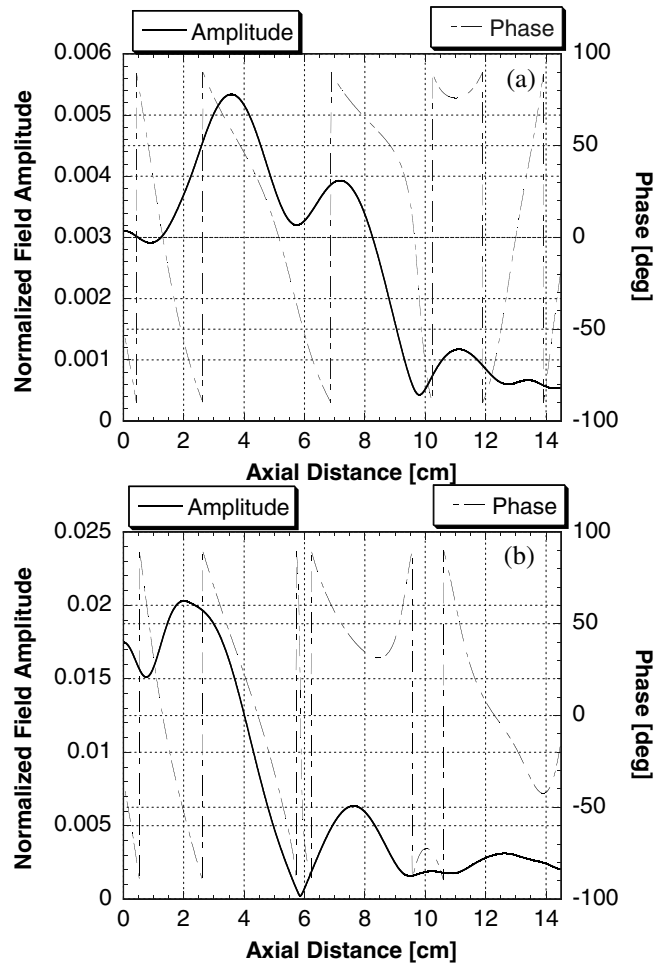


FIG. 4. Axial structure of the wave envelope amplitude (solid lines) and phase (dashed lines) in the gyro-BWO with $R_t = 2.72$ mm at $I_b = 0.1$ A (a) and 1.5 A (b).

show a qualitative agreement with the tapered waveguide results of Fig. 3. Namely, a zone of stable operation can form at higher currents than in the case of the zero reflection coefficient. Further, this behavior persists when the waveguide transition at the beam exit is made to be very gradual. In this case it can be presumed that there is no wave reflection at the beam exit. Thus, the effect of reflection at the entrance is not to increase the quality factor of the cavity but, rather, to provide for a forward wave with which the beam interacts. A complicating factor in our interpretation is the fact that for the tapered waveguide the reflection coefficient is frequency dependent. Signals close to cutoff are more strongly reflected than those that are not. Further, as the beam current is raised the natural oscillation frequency is pulled up. For example, for $R_t = 2.74$ cm the oscillation frequency increases by about 0.4 GHz and the reflection coefficient decreases from 0.7 to about 0.04 as the current increases from 1.5 to 10 A. Thus, this means that in the plane shown in Fig. 3 the reflections depend not only on the radius of the taper (horizontal axis) but also on the beam current (vertical axis). This effect is especially

well pronounced when the device operates near cutoff (gyromonotron regime).

All of the results presented above were obtained for an external magnetic field value 14.52 kG which corresponds to excitation of the backward wave. (For the TE₁₁ wave excited in a circular waveguide of 2.65 mm radius by a 100 kV electron beam, the excitation at the cutoff occurs when the external magnetic field is equal to 14.166 kG.) To analyze the transition from the operation in the gyro-BWO regime to the gyromonotron operation, we carried out simulations for magnetic fields in the range from 14.52 to 14.22 kG. Axial structures of the excited fields in the regular waveguide ($R_t = 2.65$ mm) are shown in Fig. 5. Structure (a) in Fig. 5 is the axial structure for the case $B_0 = 14.52$ kG, $I_b = 0.06$ A. In this case the device exhibits the onset of stationary oscillations of the backward-wave mode with three axial variations. Decreasing the magnetic field from 14.52 to 14.42 kG greatly changes the axial structure of the mode to the one shown by curve 5(b); so, this is the mode with one axial variation only. Simultaneously, the transition to stationary oscillations takes a longer time (more than 100 ns, while, when $B_0 = 14.52$ kG, it takes about 50 ns only). To explain this fact, let us recall that the starting current is proportional to the wave group velocity

$$v_{gr} = \frac{d\omega}{dk_z} = c^2/v_{ph} = c^2k_z/\omega \quad (1)$$

(here ω , k_z , and $v_{ph} = \omega/k_z$ are the wave frequency, axial wave number, and phase velocity, respectively). Therefore, by lowering the magnetic field we decrease the axial wave number and the starting current and thus increase the I/I_{st} ratio, which makes stationary oscillations less stable.

A further lowering of the magnetic field does not change the axial structure drastically as shown by curves (c) and (d) in Fig. 5. Both figures are given for $B_0 = 14.22$ kG but for different currents. Case 5(c) corresponds to the same 60 mA current as previously; however, at these mag-

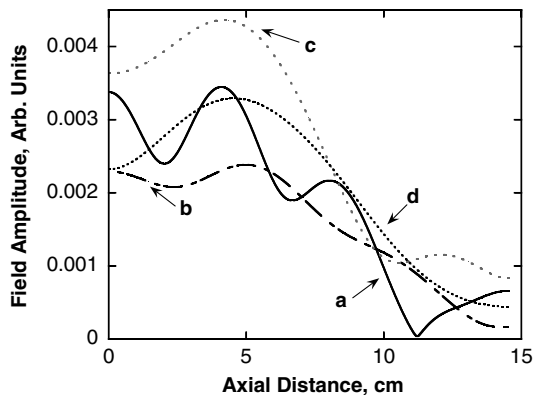


FIG. 5. Transition from the gyro-BWO to the gyromonotron operation: modification of the axial structure with the external magnetic field decrease.

netic fields and beam currents there is a weak automodulation. This automodulation disappears at 30 mA, which is case 5(d).

In summary, the presence of reflections at the beam input end of a tapered gyro-BWO allows for the operation with currents exceeding the start current by many orders of magnitude. In the absence of such reflections the device becomes unstable at a few times the start current just as does a linear beam BWO. The effect appears to result from the simultaneous interaction of the beam with both the forward and the backward waves. Such interaction is possible because the gyro-BWO operates close to cutoff and the Doppler shift is small. Similarly, there is a continuous transition from the gyro-BWO operation to the gyromonotron operation as the magnetic field is varied.

The results obtained clearly indicate that further optimization of the gyro-BWO operation should primarily be focused on the design of the input tapered section. Note that in the process of this optimization not only the efficiency enhancement and the stability of operation but also the issue of frequency tunability can be addressed. Similar tapering can also be used for improving stability of high-power gyrotrons operating in higher-order modes. As known [14], such gyrotrons are used for electron cyclotron plasma heating, current drive, and suppression of plasma instabilities in controlled fusion reactors.

This work was supported by the Multidisciplinary University Research Initiative on Vacuum Electronics sponsored by the Air Force Office of Scientific Research. The authors would like to acknowledge the interest of K. R. Chu and O. Dumbrajs in their work.

-
- [1] G. S. Nusinovich and O. Dumbrajs, *IEEE Trans. Plasma Sci.* **24**, 620 (1996).
 - [2] S. H. Chen, K. R. Chu, and T. H. Chang, *Phys. Rev. Lett.* **85**, 2633 (2000).
 - [3] F. S. Rusin and G. D. Bogomolov, *JETP Lett.* **4**, 160 (1966).
 - [4] D. E. Wortmann and R. P. Leavitt, in *Infrared and Millimeter Waves*, edited by K. Button (Academic Press, New York, 1983), Vol. 7, Chap. 7, Pt. II, p. 321.
 - [5] C. S. Kou *et al.*, *Phys. Rev. Lett.* **70**, 924 (1993).
 - [6] N. S. Ginzburg, S. P. Kuznetsov, and T. N. Fedoseeva, *Radiophys. Quantum Electron.* **21**, 728 (1979).
 - [7] B. Levush *et al.*, *IEEE Trans. Plasma Sci.* **20**, 263 (1992).
 - [8] B. P. Bezruchko, S. P. Kuznetsov, and D. I. Trubetskov, *JETP Lett.* **29**, 162 (1979).
 - [9] D. Ruelle and F. Takens, *Commun. Math. Phys.* **20**, 167 (1971).
 - [10] V. K. Yulpatov, *Sov. Radiophys. Quantum Electron.* **10**, 471 (1967).
 - [11] N. S. Ginzburg, G. S. Nusinovich, and N. A. Zavolsky, *Int. J. Electron.* **61**, 881 (1986).
 - [12] M. Botton *et al.*, *IEEE Trans. Plasma Sci.* **26**, 882 (1998).
 - [13] H. R. Johnson, *Proc. IRE* **43**, 684 (1955).
 - [14] K. L. Felch *et al.*, *Proc. IEEE* **87**, 752 (1999).